PNAS RESEARCH ARTICLE | PLANT BIOLOGY

In situ cavitation bubble manometry reveals a lack of light-activated guard cell turgor modulation in bryophytes

Craig R. Brodersen[a,1], Tim J. Brodribb[b], Uri Hochberg[c], N. Michele Holbrook[d], Scott A. M. McAdam[e], Joseph Zailaa[a], Brett A. Huggett[f], and Philippe Marmottant[g]

Affiliations are included on p. 7.

Edited by Dominique Bergmann, Stanford University, Stanford, CA; received October 10, 2024; accepted January 23, 2025

Diversification of plant hydraulic architecture and stomatal function coincides with radical changes in the Earth's atmosphere over the past 400 my. Due to shared stomatal anatomy with the earliest land plants, bryophyte stomatal behavior may provide insights into the evolution of stomatal function, but significant uncertainty remains due to technical limitations of measuring guard cell turgor pressure in situ. Here, we introduce a method for monitoring cell turgor pressure by nucleating microbubbles within the guard cells of intact plant tissue and then examining microbubble growth and dissolution dynamics. First, we show that maximum microbubble radius decreases with increasing pressure as the pressure of the surrounding fluid constrains its growth according to a modified version of the Epstein–Plesset equation. We then apply this method to monitor turgor pressure in dark- vs. light-acclimated guard cells across bryophyte taxa with stomata, where their role in gas-exchange remains ambiguous, and in vascular plants with well-documented light-dependent turgor modulation. Our findings show no light-activated change in turgor in bryophyte guard cells, with pressures not significantly different than neighboring epidermal cells. In contrast, vascular plants show distinct pressure modulation in response to light that drives reversible changes in stomatal aperture. Complete guard cell turgor loss had no effect on bryophyte stomatal aperture but resulted in partial or complete closure in vascular plants. These results suggest that despite conserved stomatal morphology, the sampled bryophytes lack dynamic control over guard cell turgor that is critical for sustaining photosynthesis and inhibiting desiccation.

stomata | bryophyte | turgor pressure | vascular plant | guard cells

Significance

Stomatal evolution was a primary driver in the radical transformation of Earth's atmosphere over the past 400 my, providing plants with the ability to regulate water loss and optimize photosynthesis. Modulating guard cell turgor pressure was a key innovation, which may be unique to vascular plant lineages. However, interrogating cell turgor pressure remains challenging and limits our ability to understand the evolution and diversity of stomatal behavior. Here, we present a method to estimate changes in epidermal cell turgor pressure in situ by nucleating cavitation microbubbles inside epidermal cells and observing their dynamics using a high-speed camera. This study shows that vascular plant guard cells increase their turgor pressure in response to light, while nonvascular plant stomata fail to respond.

Stomata are microscopic cellular valves that regulate the flux of CO_2 and water vapor across the plant epidermis. The first unequivocal evidence of structures anatomically similar to extant stomata appears in the late Silurian near the reproductive structures of *Cooksonia* (1). Today, every major terrestrial plant lineage except the liverworts possesses stomata (2–4). Control of stomatal aperture, along with a suite of other key hydraulic traits [including the cuticle, roots, and vascular system (1)], enables homiohydry (5), the ability to regulate plant water status in response to environmental conditions. The evolution of stomata and the complex physiological regulation of these dynamic pores was key to the evolutionary success of land plants (6–8), radically changing the terrestrial landscape and atmosphere (9, 10).

While most terrestrial land plants share the same superficial stomatal anatomy regardless of their placement on the plant body (3), significant uncertainty and debate exist regarding the functional role of stomata in bryophytes (11, 12). A focus on bryophyte stomata is motivated by the possibility that extant bryophytes, sister to vascular plants, may preserve some features of ancestral stomatal physiology of the morphologically similar ancestors of land plants(11, 13). Vascular plant stomata can be found at high densities on leaves (>100 stomata per mm^2) where they support photosynthetic gas exchange. In contrast, bryophyte stomata occur at very low densities and are restricted to the base of the sporophyte capsule in mosses, or distributed along the developing sporophyte in hornworts (4, 14), a placement similar to the stomatal arrangement in early land plants (1). Upon sporophyte maturation, bryophyte stomata irreversibly open, exposing the surrounding tissue to the dry atmosphere (15–18). Sporangia then rapidly dehydrate and release spores (15). Mutant moss plants incapable of developing stomata show delayed spore maturation and release (15). Whether bryophyte stomata regulate stomatal aperture to support photosynthesis during the early stages of sporophyte development remains equivocal (6, 11, 12, 17–24).

Regulation of stomatal aperture in extant vascular plants is highly conserved, whereby an increase in the turgor pressure of the guard cells mechanically forces them to bend

Author contributions: C.R.B., T.J.B., U.H., N.M.H., and S.A.M.M. designed research; C.R.B., T.B., and P.M. performed research; C.R.B. and P.M. contributed new reagents/analytic tools; C.R.B., J.Z., B.A.H., and P.M. analyzed data; and C.R.B., T.J.B., U.H., N.M.H., S.A.M.M., J.Z., B.A.H., and P.M. wrote the paper.

Competing interest statement: C.R.B. and Yale University filed a US patent application covering the conceptual ideas of the CBM method.

This article is a PNAS Direct Submission.

[1]To whom correspondence may be addressed. Email: craig.brodersen@yale.edu.

This article contains supporting information online at https://www.pnas.org/lookup/suppl/doi:10.1073/pnas.2419887122/-/DCSupplemental.

Published March 26, 2025.

apart, creating the stomatal pore through which gasses can diffuse (25–27). This process relies on the guard cells both responding to environmental stimuli, such as light, and regulating turgor pressure independently of the surrounding epidermal cells. Environmentally responsive stomata enable plants to maximize photosynthesis under favorable conditions, yet conserve water during periods of darkness or drought, thereby providing a sophisticated means of interacting with the environment.

Two competing lines of thought exist regarding the evolution of stomatal function (6, 11, 19, 28). The first is that stomatal anatomy evolved in conjunction with the suite of functional traits that allowed early land plant stomata to operate much in the same way as extant seed plant lineages, showing sensitivity to light, CO_2, vapor pressure deficit, and the hormone abscisic acid (19, 24, 29). This view places the evolution of complexly regulated stomata at or near their origin in the late Silurian (30) and implies that stomata located on sporangia or gametangia of the first stomatophytes, and the ancestor to both bryophytes and vascular plants, played a significant role in regulating photosynthetic gas exchange.

A second interpretation is that the evolution of the physiological machinery connecting stomatal function with photosynthetic gas exchange did not evolve in the ancestor of land plants. Rather, selection for novel innovations in this machinery over time has played an important role in the evolution of the major vascular plant clades (12, 31, 32). For example, associating stomata to the sporophytic, photosynthetic lamina (i.e., the leaf) and then modulating the flux of ions across the guard cell plasma membrane in response to endogenous and environmental signals, vascular plants evolved the capacity to drive reversible changes in guard cell turgor relative to the surrounding epidermal cells, and thereby modulate stomatal aperture (26).

Large among the uncertainties that limit conclusive resolution of the stomatal evolutionary debate is the action of bryophyte stomata and their response to environmental stimuli (21, 22, 30, 33). Given the size of these plants and the few stomata they possess, all data on stomatal function in this group of land plants to date are based on imprecise proxy measurements for changes in stomatal turgor pressure, either as whole organ gas exchange measurements or stomatal aperture measurements in isolated sporophyte tissue. Because of the extremely low gas fluxes between the bryophyte sporangium and atmosphere and the difficulty in accurately measuring stomatal aperture, progress in establishing whether bryophyte stomata are turgor operated valves capable of reversibly changing aperture remains problematic.

A critical component for better understanding guard cell physiology broadly, and specifically within the context of the diversification of stomatal function, is the direct measurement of guard cell turgor. Existing methods are confounded by limitations of scale, invasiveness, and throughput. Direct pressure-probe methods are restricted to species with exceptionally large guard cells (34, 35), where technically challenging micromanipulation of the probe and successful impalement of the target cell results in low sample yield. Indirect methods, such as ball tonometry (36) or microindentation have yet to be demonstrated on intact plant tissues (37). Here, we describe a method to determine guard cell pressure that overcomes many of these limitations.

Results

Cavitation Microbubble Dynamics as a Proxy for Cell Turgor Pressure. Our method, hereafter referred to as the cavitation bubble manometer (CBM; Fig. 1), provides a proxy measurement of cell turgor pressure based on the dynamics of cavitation bubbles nucleated in guard cells or epidermal cells of intact plants. The method is noninvasive, requires no sample preparation, can be used with actively transpiring plants, and has a potential throughput of >50 measurements per day. The CBM is composed of laser ablation components used to study developmental biology of plant (38) and animal (39) systems, but modified to nucleate microbubbles in plant cells without damage. Microbubbles nucleated in guard cells or epidermal cells behave as predicted by a modified version of the Epstein–Plesset equation [(40); Fig. 1*D*], where the pressure of the surrounding liquid constrains the maximum microbubble radius. We employ high-speed imaging and a simple image processing routine to extract the salient cavitation microbubble dynamics related to turgor pressure (Fig. 1*D*).

Assuming a common mechanism across all taxa with morphologically similar guard cell anatomy (where an increase in pressure deforms the shape of guard cells to open the pore) then guard cell turgor pressure should increase in response to a universally important environmental signal for terrestrial photosynthetic plants: light intensity. Responding to light was likely one of the earliest selective pressures driving the evolution of stomatal regulation (8), resulting in stomatal opening during the day to allow CO_2 to enter the plant to sustain photosynthesis, and closure for water conservation at night or during water deficit. Therefore, in taxa with stomata that actively respond to light, we would expect guard cell turgor pressure to increase after a transition from dark to light. This would manifest as a reduction in microbubble maximum radius and dissolution time compared to those in the dark and in nearby epidermal cells.

We first generated microbubbles in epidermal cells and guard cells of dark-acclimated plants and monitored microbubble growth and dissolution dynamics (Fig. 1*E* and Movie S1). We then exposed the same plants to light for at least 30 min and repeated the experiment (Fig. 1*F* and Movie S2). Confirming the sensitivity of the method, we observed that microbubbles were smaller and dissolved faster in light-acclimated guard cells compared to dark-acclimated guard cells, i.e., when pressure was expected to be high and low, respectively, in a representative angiosperm species (*Senecio minimus* Poir. Asteraceae; Fig. 1 *E*–*G*). Guard cell movements in *S. minimus*, with a guard cell length of approximately 40 to 50 μm, were unambiguous allowing for accurate measurement of stomatal aperture. Repeated microbubble dynamics observed in the same guard cells over time transitioning from high to low light showed an increase in maximum microbubble radius and dissolution time (Fig. 1*H*), indicating a decrease in turgor pressure as the aperture closed.

Light Exposure Fails to Induce Turgor Change in Three Bryophytes. To test whether bryophyte guard cells respond to light, we measured microbubble dynamics in guard cells and epidermal cells from immature capsules of two mosses (*Funaria hygrometrica* Hedw. Funariaceae; *Leptobryum pyriforme* (Hedw.) Wilson Bryaceae) and green regions of hornwort sporophytes (*Phaeoceros carolinianus* (Michx.) Prosk. Notothyladaceae) and then compared them to microbubbles generated in microphylls of a lycophyte (*Selaginella kraussiana* (Kunze) A.Braun Selaginellaceae), pinnae of two ferns (*Polystichum proliferum* (R.Br.) C.Presl., Dryopteridaceae; *Adiantum aethiopicum* L., Pteridaceae), and leaves of two angiosperms (*Arabidopsis thaliana* (L.) Heynh. var. Col-0, Brassicaceae; and *S. minimus*). All leaves, microphylls, or sporophytes remained attached to the plant during measurements, and plants were kept in a well-hydrated state.

We found no significant change in maximum microbubble radius (Fig. 2 *A* and *C*) or dissolution time (*SI Appendix*, Fig. S1 *A*–*C*) in response to light for either cell type in the sampled bryophytes. In

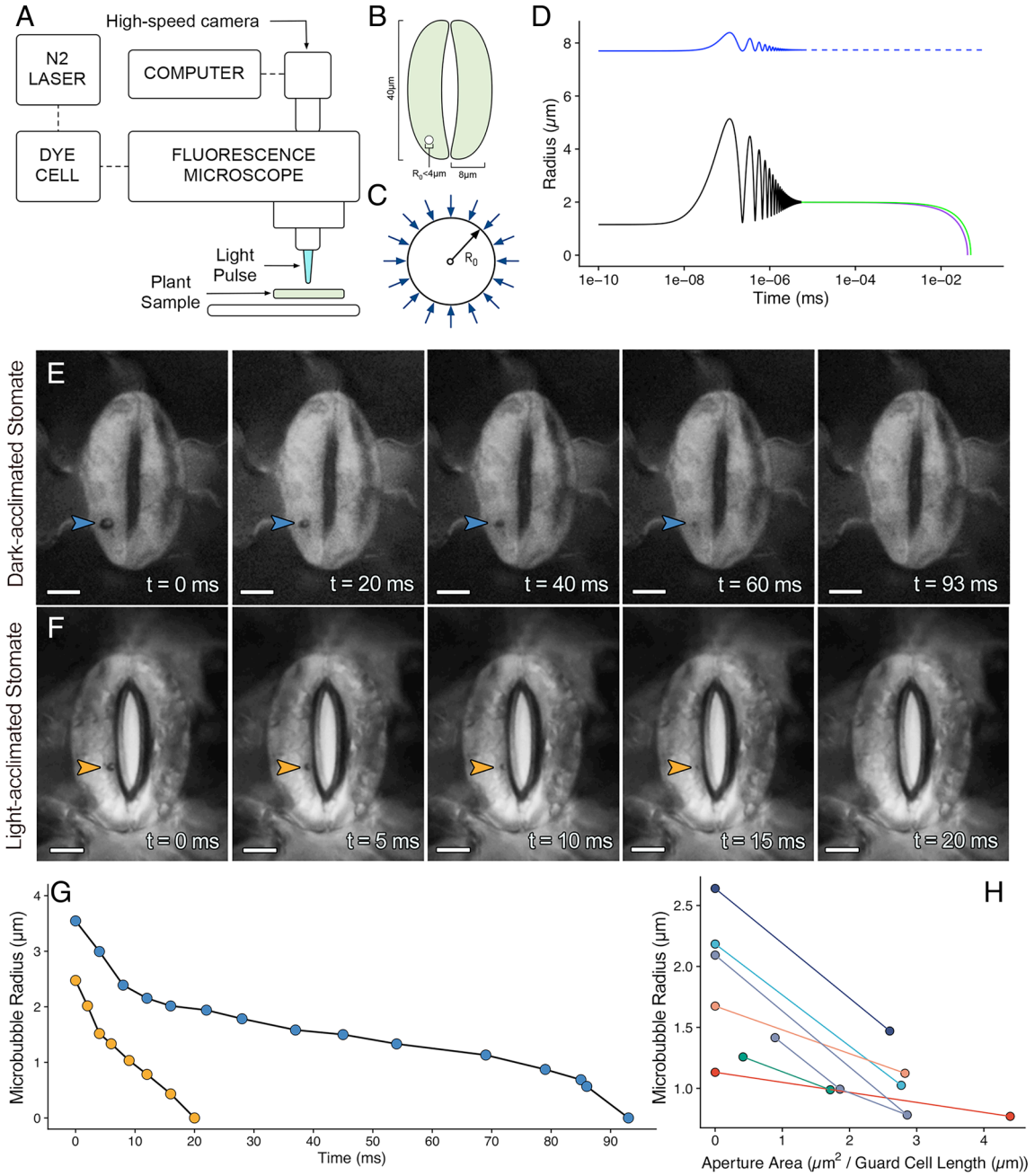

Fig. 1. Estimating guard cell turgor with the CBM. (*A*) The CBM is constructed from a modified laser ablation system coupled to a compound microscope and high-speed camera. (*B*) The CBM delivers a ns pulse of light energy focused inside a plant cell which nucleates a microbubble inside a target cell, in this case epidermal cells or stomatal guard cells. (*C*) Theory and empirical data show that maximum microbubble radius is dependent pressure of the surrounding fluid which constrains microbubble expansion Eq. **1** in the text. (*D*) Predicted dissolution time of a microbubble with a radius of 2 μm using Eq. **2** is within the general range of observable microbubbles nucleated inside plant cells with the CBM. (*E* and *F*) Representative frames from time-lapse image sequences of microbubble dissolution in closed (*E*) or open (*F*) *Senecio minimus* stomata. Arrows in *E* and *F* point to the microbubble generated with the CBM (Scale bar, 10 μm). In (*E*), the microbubble is no longer visible in the final frame, making the total dissolution time 93 ms. (*F*) shows a time-lapse sequence of microbubble dissolution in an open stomate, where higher turgor pressure yields a smaller maximum bubble radius and faster dissolution time, 20 ms. (*G*) Radius vs. time plots for microbubbles in an open guard cell (orange) and closed guard cell (blue). (*H*) In *S. minimus*, increasing aperture area leads to smaller maximum microbubble radii indicating higher pressure. Points with the same symbol color represent repeated measurements on the same guard cell after being exposed to light.

contrast, microbubble radii in light-acclimated guard cells of vascular plants were significantly smaller (Fig. 2 *D* and *H*) and dissolved faster than microbubbles in dark-acclimated stomata (*SI Appendix*, Fig. S1 *D* and *H*). These data are consistent with a light activated increase in guard cell pressure to force stomata open in vascular plants, and a lack of this response in the three sampled bryophytes. In *S. minimus*, stomatal opening in the light also resulted in concurrent increased apparent turgor pressure in the epidermal cells, but not a significant change in the dissolution rate (*SI Appendix*, Fig. S1*G*). This is likely because of the displacement volume of the large guard cells in this species encroaching upon the neighboring epidermal cells, which have considerable mechanical advantage (41).

Stomatal Turgor Pressure Associated With Sporangium Development in Bryophytes. Microbubbles did not dissolve in guard cells from the moss *F. hygrometrica* after the operculum had turned brown (*SI Appendix*, Fig. S2*A*). Instead, microbubbles could be generated but their shape was often aspherical and they would not dissolve, indicating a highly viscous consistency of

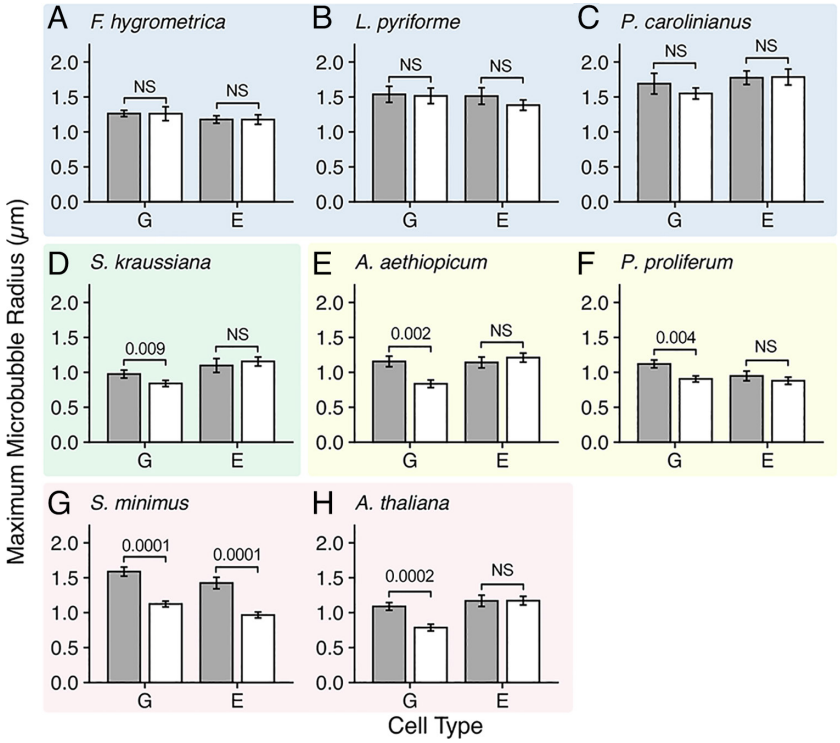

Fig. 2. Maximum mean microbubble radii generated with the CBM in epidermal and guard cells used as a proxy for cell turgor pressure in three bryophytes (*A*–*C*; blue shading), a lycophyte (*D*; green shading), two ferns (*E* and *F*; yellow shading), and two angiosperms (*G* and *H*; red shading). Plant tissues were dark-acclimated (gray bars) and then transitioned to the light (white bars) with CBM measurements under both light treatments. Microbubble radius was not significantly different in guard cells (bars marked *G*) acclimated to the light and dark in the bryophytes, indicating no change in turgor pressure. Microbubble radius decreased significantly ($P < 0.05$) in all vascular plant taxa (*D*–*H*), indicating increased turgor pressure in response to light exposure which forces stomata to open. Epidermal cells (bars marked *E*) serve as a paired reference point for each species, which did not change significantly in any species in response to light except *S. minimus*. Data are represented as mean ± SEM. N > 10 for all cell types and treatments.

the cytoplasm due to excessive water loss or low water content. This suggests that as capsules develop the guard cells lose turgor but retain their general shape. Similarly, we found that in the hornwort *P. carolinianus*, microbubbles dissolve quickly in guard cells from the green basal regions near the involucre but did not dissolve in the distal regions beyond the transition zone where the sporophyte turns brown (*SI Appendix*, Figs. S2 *B*, *C*, and S3). Within the green basal regions, stomata closer to the involucre exhibited smaller microbubble radii and more rapid microbubble dissolution compared to more distal cells (*SI Appendix*, Fig. S3). The rigid cellular structure of epidermal and guard cells in these taxa likely preserve their turgid appearance despite the loss of turgor. This makes it inherently difficult to infer functional status from an observation of aperture alone.

Rapid Turgor Loss Does Not Change Bryophyte Stomatal Aperture. We next modified the CBM to test the effect of turgor loss on stomatal aperture. An open stomate experiencing rapid pressure failure should lead to closure, observable as a reduction in aperture. Increasing the power of the laser allowed us to cause an instantaneous catastrophic loss in turgor pressure, presumably due to rupture of the cell wall and plasma membrane, similar to the classical experiments by Heath, where guard cells were impaled with a glass needle to achieve the same result (42). After allowing plants to acclimate to light we identified stomata that appeared to be open (Fig. 3), and then monitored stomatal aperture following a catastrophic pulse of energy indicated by rapid (<100 ms) changes in guard cell position or the formation of a large (>5 μm) diameter microbubble that increased in volume and displaced the cellular contents (Fig. 3). These microbubbles were distinctly different from the rapidly dissolving microbubbles used to monitor turgor, in that they persist and grow rather than dissolve. Microbubble growth indicates that liquid pressure surrounding the bubble had fallen below the pressure inside the bubble (43, 44). Persistence and growth of these bubbles can be interpreted as the remaining liquid surrounding the bubble being in contact with the apoplast due to the ruptured membrane. The apoplastic solution should be under tension, and thereby counteract the effects of surface tension and internal gas pressure acting on the liquid–vapor boundary of the microbubble (45).

We observed negligible changes (i.e., within the margin of measurement error) in stomatal aperture in all three bryophyte species following a membrane-damaging event (Fig. 3 *A*, *B*, and *I*). In contrast, rapid loss of turgor resulted in stomatal closure in all five vascular plants. Complete closure of the pore was observed in the lycophyte and ferns (Fig. 3*I*) even though only one guard cell in the pair was damaged. This is because plasmodesmata hydraulically link the guard cell pair (46), such that damage or loss of turgor in one guard cell compromises the hydraulic integrity of its partner. The effect of this hydraulic coupling is illustrated with this method and differs from the behavior of the angiosperms. Similar to the results of Heath (42), we found that the aperture of stomata in both angiosperms was reduced by ca. 50% (Fig. 3*I*), showing that angiosperm guard cells are not hydraulically linked.

Discussion

The CBM method has potential to reveal physiological processes at the cellular level as evidenced by our conclusive demonstration of nonhomology in guard cell behavior in our sampled bryophytes and vascular plants. Plant cell turgor pressure is an essential

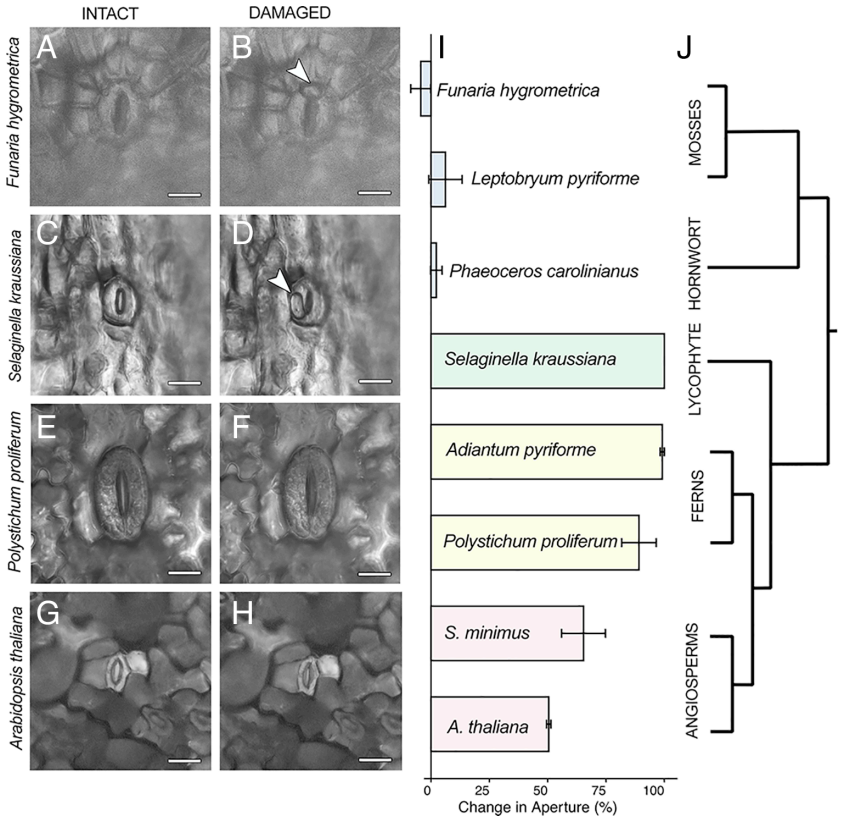

Fig. 3. Percent change in stomatal aperture resulting from an artificially imposed rapid loss of guard cell turgor generated using a high energy pulse from the CBM which damages the integrity of the cell membrane. Resulting damage leads to no change in aperture in bryophyte stomata, complete stomatal closure in a lycophyte and ferns, and partial closure in vascular plants. Paired representative images of stomatal aperture before (*Left* image column) and after a rapid loss in turgor (*Right* image column) (*A*–*H*) in a bryophyte (*F. hygrometrica*; *A* and *B*), lycophyte (*S. kraussiana*; *C* and *D*), fern (*P. proliferum*; *E* and *F*), and angiosperm (*A. thaliana*; *G* and *H*). Mean change in stomatal aperture (*I*) for all studied taxa aligned with a generalized phylogeny (*J*). Turgor loss is indicated in taxa with no change in aperture due to the presence of an expanding microbubble (white arrow). (Scale bar, 10 μm.)

physiological trait that is difficult to measure in transpiring tissues. The number of published in situ guard cell turgor pressure measurements is <30, arriving from only two studies, and from just two species with large guard cells that are easy to probe(47, 48). All other measurements are from detached tissue and typically submerged in a bathing solution, thereby removing those tissues from their natural state. Here, we report 466 in situ pressure measurements from eight diverse taxa across two cell types, highlighting the significant advancement in access to cell turgor and the CBM's high-throughput capability. Notably, these measurements can now be used in plants with stomata too small to interrogate with a cell pressure probe (25), such as in the model system *A. thaliana* and the many mutant lines available for investigating guard cell physiology. Furthermore, we demonstrate that the same tissue, and in some cases even the same guard cells, can be repeatedly measured over time as they respond to environmental stimuli. Given the increase in the number of new model plant taxa, including bryophytes with capabilities for gene manipulation (49–51), the versatility of the CBM and its amenability to diverse taxa represent a major advancement in the available toolkit for studying plant cell physiology and evolution.

Limited and equivocal published data are available on the responsiveness of bryophyte guard cell responses to light (19). Two studies report light-responsive guard cells in bryophytes (*F. hygrometrica* and *Physcomitrium patens*), and both studies used aperture measurements to support this claim (21, 33). Meanwhile, aperture (22), developmental (20), and gas exchange (17) data suggest a lack of a light-activated response. Stomatal response to other cues, such as ABA or CO_2, remain similarly uncertain, with reports for and against environmentally responsive stomata in bryophytes, often in the same taxa (19). Our data (Figs. 2 and 3 and *SI Appendix*, Figs. S2 and S3) strongly support the view that there is no active regulation of guard cell turgor in response to light in bryophyte stomata, and that mechanical stresses arising due to volume shifts in adjacent tissues during sporophyte desiccation lead to permanent stomatal opening (20). Data that support bryophyte stomata as responsive to environmental stimuli come from observations made early in sporophyte development (21, 33). Our in situ measurements during this same developmental stage show no turgor changes in response to light, and no difference in turgor compared to the neighboring epidermal cells. The minute changes in stomatal aperture in response to environmental cues reported in these studies (24, 33) were not performed on the same stomate or even the same tissue samples under different conditions.

In contrast, the CBM has allowed us to collect data on the same tissues within a few hours of dark- or light-acclimation. Because of the three-dimensional nature of moss sporangia (1, 26), stomatal aperture is difficult to observe and measure accurately in situ, and thus in most cases requires destructive methods (21, 52). This leads us to believe that previous reports of active stomatal regulation in bryophytes are likely due to a misinterpretation of developmental status, the result of errors in focusing on a consistent plane through the pore, or artifacts of using epidermal surface impressions. These concerns call into question (24, 33, 52) studies that report bryophyte stomata as responsive to environmental stimuli and suggest that techniques dependent upon direct aperture measurement are highly problematic for inferring function. Furthermore, the irreversible opening of bryophyte stomata during the later stages of sporophyte development are in direct contrast to stomatal function in vascular plants, particularly in the context

of poikilohydry as a general rule in the bryophytes vs. homiohydry in vascular plants (5).

Our in situ measurements of epidermal and guard cell turgor across eight diverse taxa represents a significant advancement in our basic understanding how plant cell turgor pressure is modulated in response to environmental factors and highlights a crucial transition in the accessibility of biophysical processes that are essential for all plant cells. The technique allows for the examination of cells in transpiring tissue and is compatible with model systems, such as *A. thaliana* and accompanying genetic resources. With its high-throughput capacity, the CBM facilitates the investigation of the biomechanics and physiological principles of guard cell movements and the coordination of aperture with the surrounding epidermal cells.

Materials and Methods

Overview of the CBM. We constructed the CBM from a modified laser ablation system (Micropoint, Andor, Concord, MA, USA) and compound fluorescence microscope (Olympus BX43; Tokyo, Japan) to generate a focused pulse of light (466 nm) with a radius of ~2.5 μm inside a target cell on the plant epidermis (Fig. 1 *A* and *B*). The output power was attenuated from 1.3 to 0.45 μJ with a neutral density gradient filter. A 20x long-working distance objective (Olympus SLMPLN) was used to focus light from the system and for observation. The energy pulse nucleates microbubbles with a radius of <4 μm inside the target cell, which typically grow and dissolve within <250 ms. Observations of microbubble radius and dissolution time in angiosperm leaves were concordant with established theory and experimental work in physical systems (53, 54), which justified the application of this method to other taxa to test whether modulation in guard cell turgor could be interrogated with the CBM. To test the hypothesis that if stomata from representative bryophyte taxa are nonfunctional, then microbubble radius, and therefore guard cell turgor, would remain unchanged in response to light, we conducted cell-specific experiments on tissues to dark and light conditions. In contrast, we predicted that in vascular plants epidermal cell turgor would remain constant, while guard cell turgor would increase in response to light, indicated by a decrease in microbubble radius. Full details on our methods are available in *SI Appendix*.

Theoretical Model for Maximum Microbubble Radius. Microbubble growth and dissolution dynamics in artificial systems provide a robust theoretical basis for our method (54–56), where increasing pressure of the surrounding liquid constrains the maximum microbubble radius [Fig. 1*C*; (55)]. We assume that the laser converts a number of molecules, n_g, to the gas phase, independently of the value of pressure in the liquid P_0. At equilibrium, which occurs just after the initial oscillations described in the next section are damped, the gas pressure given by the ideal gas law is balanced by the liquid pressure through the Young–Laplace equation $p_g = n_g RT/V = P_0 + 2\sigma/R_0 + KV/V_{cell}$, where σ is surface tension, K is the cell+water expansion modulus and V_{cell} the guard cell volume. We will see later that both the surface tension and expansion terms are negligible. Therefore, the maximal bubble radius observed by the camera (that cannot capture initial oscillations) is predicted to be

$$R_{max} = \left(\frac{3n_g RT}{4\pi P_0}\right)^{1/3}. \quad [1]$$

Theoretical Model for Microbubble Nucleation, Oscillations, and Dissolution. We model the dynamics of a bubble of radius R assuming a spherical geometry for the guard cell of volume V_{cell}. We introduce the effective cell radius R_c such that $V_{cell} = 4/3 \times \pi R_c^3$. An important parameter is the extensibility of the cell volume, measured by the expansion modulus $K_{cell} = V_{cell} dP/dV_{cell}$. Typical values from *Vicia faba* guard cells (25) indicate a V_{cell} of 4,000 to 5,000 μm^3, with K_{cell} on the order of $8-12$ MPa at a turgor pressure of 1 MPa and then increasing linearly with pressure. This value for K_{cell} is much less than the bulk modulus of water itself ($K_{water} = 2.2$ GPa, two orders of magnitude higher).

The dynamical evolution of confined bubbles was studied by Vincent et al. (56) for the case of a centered bubble. For a very small bubble adjacent to R_c, the equation for the evolution of the radius is

$$R\frac{d^2R}{dt^2} + \frac{3}{2}\left(\frac{dR}{dt}\right)^2 = \frac{1}{\rho_l}\left(p_g(R)\left(1-\frac{3\gamma}{c}\frac{dR}{dt}\right) - \frac{2\sigma}{R} - P_0 - K\left(\frac{R}{R_c}\right)^3\right), \quad [2]$$

with ρ_l the liquid density, σ the surface tension, P_0 the initial pressure, and $K = \left(K_{cell}^{-1} + K_{water}^{-1}\right)^{-1} \simeq K_{cell}$ the expansion modulus of the cell+water, while the gas pressure taken in adiabatic conditions to be $p_g = p_{g,0}\left(R/R_0\right)^{-3\gamma}$, with γ the adiabatic coefficient and $p_{g,0}$ and R_0 the values at equilibrium.

To account for damping, we added a term of acoustic radiation damping using the proposition of Brenner et al. (57) for the modified Rayleigh-Plesset equation valid in the extreme conditions of sonoluminescence, replacing $p_g(R)$ by $p_g(R)\left(1-3\gamma/c \times dR/dt\right)$. This addition neglects any backward reflection of the emitted acoustic waves and assumes that all the acoustic energy is radiated with sound velocity c. Earlier studies have shown that acoustic radiation damping is a major source of energy dissipation compared to viscous or thermal damping (57). The linearization of the previous oscillation for small vibration of the radius around R_0 provides the equation of a damped oscillator with a pulsation $\omega_0^2 = \left(3\gamma p_{g,0} - 2\sigma/R_0 + 3KR_0^3/R_c^3\right)/\left(\rho_l R_0^2\right)$ and a quality factor that writes $Q \simeq c/R_0\omega_0$ when the second and last term in the parenthesis of the pulsation are negligible.

The dynamical equation Eq. **2** is integrated numerically to provide the radius versus time with the following parameters: an initial nuclei radius $R = 1.15\,\mu m$ at time 0 (smaller than the equilibrium radius $R_0 = 2\,\mu m$) in a cell of radius $R_c = 7.7\,\mu m$ under pressure $P_0 = 1$ MPa, with $K_{cell} = 10$ MPa, $\sigma = 70 \times 10^{-3}$ N/m. We have the following orders of magnitude: $2\sigma/R_0 = 0.07$ MPa and $KR_0^3/R_c^3 = 0.16$ MPa. Thus, to a good approximation, we have $p_{g,0} \simeq P_0$ from equilibrium and $Q \simeq c/R_0\omega_0$. The numerical application gives the harmonic frequency $f_0 = \omega_0/2\pi = 6$ MHz and a quality factor $Q = 20$. The bubble quickly expands, oscillates for a few cycles at MHz frequency, and relaxes toward the equilibrium radius, a process that typically includes dozens of oscillations which is completed in a few μs (Fig. 1*D*). The cavity radius oscillates slightly around its initial value when the bubble oscillates. We predict this oscillation by assuming that the liquid volume around the bubble does not change, leading to $R_c^3 = R_{c,0}^3 + R^3$.

Dissolution. At longer times, such as the ones captured by the camera operating at an image every 1 ms, the dissolution of the air bubble obeys the model by Epstein–Plesset (40),

$$\frac{dR}{dt} = \frac{-D\left(c_s - c_i\right)}{\rho_g}\left[\frac{1}{R} + \frac{1}{(\pi Dt)^{1/2}}\right], \quad [3]$$

with $D = 2 \times 10^{-9}$ m^2/s the diffusion constant of air in the liquid, ρ_g the density of the gas, and c_s the concentration at saturation of gas ($c_s/\rho = 0.02$ for air, according to Henry's law) while c_i is the initial concentration of gas in the liquid. Surface tension was neglected for simplification, but it can accelerate dissolution, especially in the final stages. Surface tension can be accounted for using the full model given by Epstein–Plesset (40) to perform a numerical integration. The second term in Eq. **2** is quickly negligible and the approximate solution of this equation is

$$\frac{R}{R_0} = \sqrt{1 - \frac{2D\left(c_s - c_i\right)}{\rho R_0^2}t}, \quad [4]$$

meaning the dissolution time is

$$t = \frac{\rho R_0^2}{2D\left(c_s - c_i\right)}. \quad [5]$$

Model Application and Experimental Work. Plant material was mounted to a clear microscope slide using adhesive tape, and additional sample mounting varied depending on the experiment (see below). For leaves, the abaxial side was faced upward so that the leaf surface bearing stomata could be observed. Epidermal or guard cells were brought into focus and monitored with a digital camera (model #acA640-750um, Basler, Inc., Exton, PA) using the micromanager (58) plugin for the Fiji software package (59). The camera was capable of recording at 500 to 1,000 frames per second. Transmitted light from the microscope necessary for imaging at this framerate was ~1,200 μmol m^{-2} s^{-1} PPFD (photosynthetic

photon flux density) incident at the plant tissue surface. By simultaneously triggering the camera and the laser, we were able to nucleate microbubbles in the target cells and capture microbubble growth and dissolution. Locating a suitable guard cell, focusing, and acquiring and image sequence of ca. 1,000 images (i.e., 1 s of data) takes ca. 20 s, thereby limiting the total amount of time the tissue is exposed to the transmitted light illumination.

Image sequences of bubbles >10 μm radius, or bubbles that did not immediately dissolve, were discarded under the assumption that physical damage to the cell wall or membrane occurred, thereby reducing the internal turgor to a non-native value. We then analyzed the image sequences to record the maximum microbubble radius and dissolution time using ImageJ software.

Microbubble Dynamics in Guard Cells in Response to Light Stimulus. We studied fresh, intact plants from three bryophytes, a lycophyte, two ferns, and two angiosperms (*SI Appendix*, Table S1) to determine whether turgor is modulated in response to light in both epidermal and guard cells. We selected two mosses from established glasshouse populations, including *F. hygrometrica*, a model taxon that was used for stomatal aperture observations (21). We chose *S. kraussiana* for a representative lycophyte (60) that was grown in the same glasshouse. We selected *P. proliferum* and *A. aethiopicum* as representative fern taxa, which have a thin, flat lamina with easily observable stomata and epidermal cells. We then selected *Arabidopsis thaliana* var. Col-0 because of its widespread use as a model species with extensive genetic resources, and *S. minimus* because of its large guard cell size, which was comparable to those of the selected ferns (*SI Appendix*, Table S1). All plants except *A. thaliana* were grown in the same glasshouse in 0.5 L pots with a soil medium composed of a 7:4 mix of composted fine pine bark and coarse washed river sand with added 14:14:14 fertilizer (Scotts-Sierra, Marysville, OH), and maintained at 21 °C:18 °C, day:night temperatures under natural light and irrigated daily. The *A. thaliana* plants were grown from seed in 0.25 L pots in the same soil mixture and maintained in a growth chamber under 8-h daylength conditions to encourage large leaves and to inhibit flowering.

For the two mosses, *L. pyriforme* and *F. hygrometrica*, we limited our study to plants with sporophyte capsules approximately 7 to 10 d after emergence and always while the capsule was entirely green with no discoloration of the operculum which would indicate later stages of development. Our focus was on the developmental time frame where previous researchers reported stomatal aperture changes in response to light (21). We were only able to generate microbubbles that dissolved in *F. hygrometrica* guard cells prior to when the operculum turns brown (*SI Appendix*, Fig. S3), regardless of the coloration of the capsule.

To prepare the mosses for measurements, an entire plant was extracted from the soil, wrapped in moist tissue paper, and the capsule was affixed to a slide. The slide was then placed in a plastic bag with moist tissue paper and then the bag was wrapped in aluminum foil to block light >12 h. Plants were then removed from the opaque enclosure and quickly mounted on the microscope stage, at which point we started a 5 min timer. We then generated and recorded microbubble dynamics in guard cells and epidermal cells, and measurements were completed within 5 min of being exposed to the high-speed camera illumination light. Once we collected the dark-acclimated data, the slides were placed back into the plastic bag to prevent desiccation and then exposed to LED light at 250 μmol m^{-2} s^{-1} PPFD for 1 h, after which we collected a second set of light-acclimated microbubble data.

The same general procedure was performed for the hornwort *P. carolinianus*, collected from a wild population (Sandy Bay, TAS). Approximately 1 cm^2 of thallus and rhizoid tissue with sporophytes at least 2 cm long were collected and placed into a small plastic petri dish with moist tissue paper. The petri dishes were covered in foil and placed in plastic bags as above for the moss capsules. Plants remained in the petri dish with their rhizoids in contact with the moist tissue paper, but with the sporophyte affixed to a microscope slide during measurements. For a separate set of three sporophytes, we first noted the position of the involucre as a reference point and then progressed along the length of the sporophyte locating guard cells and generating microbubbles. We noted the distance from the involucre for each stomate. This process was repeated for as many stomata as possible along the length of the sporophyte until we reached the transition zone where the tissue becomes yellow/brown, after which point we were unable to produce microbubbles that would dissolve rapidly.

A similar procedure was carried out for the lycophyte *S. kraussiana*, where we selected plant segments with at least three bifurcations of the main stem with roots still attached. For the ferns and the angiosperms, potted plants were brought back to the lab and individual leaves or pinnae were sealed in plastic bags lined with aluminum foil and allowed to acclimate to the dark for at least 12 h. Microbubble dynamics were recorded for dark- and light-acclimated tissue and then the image sequences were analyzed.

We then used the resulting image sequences to also measure guard cell length and width with ImageJ to compare the dimensions between taxa (*SI Appendix*, Table S1). We determined that 250 m^{-2} s^{-1} PPFD was adequate to elicit a stomatal response in all species based on relative electron transport light response curves generated with chlorophyll fluorescence, which has been shown to be effective for bryophytes (61). Briefly, well-hydrated plants were brought to the lab and placed under a fluorescence imaging system (MINI-Imaging PAM, Walz Inc., Germany). Leaves or sporophytes were brought into focus and then we generated a light response curve from zero to 726 m^{-2} s^{-1} PPFD. We selected regions in the fluorescence images from the capsules of *F. hygrometrica* or the green portion of *P. carolinianus* sporophytes and excluded photosynthetic gametophyte or thallus tissue from the analysis. The selected value of 250 m^{-2} s^{-1} PPFD was found to be either on the initial slope or in the saturated region of the light response curve for all taxa (*SI Appendix*, Fig. S5). We measured the output spectrum of the illumination source using a spectrometer (USB-4000, Ocean Optics Inc., Orlando, FL) to confirm it produced light within 400 to 750 nm (*SI Appendix*, Fig. S6).

Response of Stomatal Aperture and Guard Cell Shape to a Rapid Loss of Turgor. In a final set of experiments, we used the light pulse from the CBM to intentionally rupture the cell membrane which led to a rapid loss of turgor in light-acclimated tissues. The neutral density filter was set to its highest-throughput position, and the guard cells were repeatedly exposed to the light pulses until large bubbles formed in the guard cells that did not immediately dissolve, or until the guard cells changed their position. This method yields similar results to those of Heath (42), but we were able to work with smaller guard cells and expand the number of taxa. We monitored guard cell position, shape, and stomatal aperture by recording images every 100 ms for approximately 2 min and repeated the experiment six times per species.

Statistics. We compared the mean bubble dissolution times between cell types (epidermal vs. guard cells) and treatments (light vs dark acclimated) using standard *t* tests and ANOVA using the dplyr package in R.

Data, Materials, and Software Availability. The data reported in this manuscript for Fig. 2 and Movies S1 and S2 are available at an online data repository, https://osf.io/n74sk/ (62). Additional data are available upon publication with a reasonable request given the large size of the total dataset.

ACKNOWLEDGMENTS. We kindly thank G. Jordan and P. Dalton for their help in identifying and sourcing species, M. Venkadesan and A. Pahlavan for discussions about the underlying physics of the method, T. Geer for technical support, and M. Hammarlund for initial experiments. The authors received research support from Newman Family Foundation for Plant Science, the Australian Research Council Centre of Excellence, and the NSF (NSF–BSF Grant #2333889; NSF #2333890).

Author affiliations: [a]School of the Environment, Yale University, New Haven, CT 06511; [b]Department of Biological Sciences, School of Natural Sciences, University of Tasmania, Hobart, TAS 7001, Australia; [c]Agricultural Research Organization, Volcani Center, Institute of Soil, Water and Environmental Sciences, Neve Ya'ar research station, Rishon LeZion 7505101, Israel; [d]Department of Organismic and Evolutionary Biology, Harvard University, Cambridge, MA 02138; [e]Purdue Center for Plant Biology, Department of Botany and Plant Pathology, Purdue University, West Lafayette, IN 47907; [f]Department of Biology, Bates College, Lewiston, ME 04240; and [g]Laboratoire de Spectrométrie Physique, UMR 5588, Université Grenoble I and CNRS, Martin d'Hères Cedex 1 F-38402, France

1. D. Edwards, H. Kerp, H. Hass, Stomata in early land plants: An anatomical and ecophysiological approach. *J. Exp. Botany* **49**, 255–278 (1998).
2. R. Ligrone, J. G. Duckett, K. S. Renzaglia, Major transitions in the evolution of early land plants: A bryological perspective. *Ann. Botany* **109**, 851–871 (2012).
3. K. S. Renzaglia, R. Joel Duff, D. L. Nickrent, D. J. Garbary, Vegetative and reproductive innovations of early land plants: Implications for a unified phylogeny. *Philos. Trans. R. Soc. London. Series B: Biol. Sci.* **355**, 769–793 (2000).
4. K. S. Renzaglia, J. C. Villarreal, B. T. Piatkowski, J. R. Lucas, A. Merced, Hornwort stomata: Architecture and fate shared with 400-million-year-old fossil plants without leaves. *Plant Physiol.* **174**, 788–797 (2017).
5. M. C. Proctor, Z. Tuba, Poikilohydry and homoihydry: Antithesis or spectrum of possibilities? *New phytol.* **156**, 327–349 (2002).
6. S. A. McAdam *et al.*, Stomata: The holey grail of plant evolution. *Am. J. Botany* **108**, 366 (2021).
7. J. A. Raven, "The evolution of vascular land plants in relation to supracellular transport processes" in *Advances in Botanical Research*, (Elsevier, 1977), **vol. 5**, pp. 153–219.

8. J. A. Raven, Selection pressures on stomatal evolution. *New Phytol.* **153**, 371–386 (2008).
9. J. A. Berry, D. J. Beerling, P. J. Franks, Stomata: Key players in the earth system, past and present. *Curr. Opin. Plant Biol.* **13**, 232–239 (2010).
10. C. K. Boyce, J.-E. Lee, Plant evolution and climate over geological timescales. *Annu. Rev. Earth Planet. Sci.* **45**, 61–87 (2017).
11. F. C. Sussmilch, M. R. G. Roelfsema, R. Hedrich, On the origins of osmotically driven stomatal movements. *New Phytol.* **222**, 84–90 (2019).
12. F. C. Sussmilch, J. Schultz, R. Hedrich, M. R. G. Roelfsema, Acquiring control: The evolution of stomatal signalling pathways. *Trends Plant Sci.* **24**, 342–351 (2019).
13. J. P. Fortin, W. E. Friedman, A stomate by any other name? The open question of hornwort gametophytic pores, their homology, and implications for the evolution of stomates *New Phytol.* **245**, 40–48 (2025).
14. E. Frangedakis *et al.*, The hornworts: Morphology, evolution and development. *New Phytol.* **229**, 735–754 (2021).
15. C. C. Chater *et al.*, Origin and function of stomata in the moss Physcomitrella patens. *Nat. Plants* **2**, 1–7 (2016).
16. J. G. Duckett, S. Pressel, K. M. P'ng, K. S. Renzaglia, Exploding a myth: The capsule dehiscence mechanism and the function of pseudostomata in Sphagnum. *New Phytol.* **183**, 1053–1063 (2009).
17. J. Kubásek, T. Hájek, J. Duckett, S. Pressel, J. Šantrůček, Moss stomata do not respond to light and CO2 concentration but facilitate carbon uptake by sporophytes: A gas exchange, stomatal aperture, and 13C-labelling study. *New Phytol.* **230**, 1815–1828 (2021).
18. S. Pressel, T. Goral, J. G. Duckett, Stomatal differentiation and abnormal stomata in hornworts. *J. Bryol.* **36**, 87–103 (2014).
19. J. W. Clark *et al.*, The origin and evolution of stomata. *Curr. Biol.* **32**, R539–R553 (2022).
20. J. G. Duckett, S. Pressel, The evolution of the stomatal apparatus: Intercellular spaces and sporophyte water relations in bryophytes--two ignored dimensions. *Philos. Trans. R. Soc. B: Biol. Sci.* **373**, 20160498 (2018).
21. D. L. Garner, D. J. Paolillo Jr., On the functioning of stomates in Funaria. *Bryologist* **76**, 423–427 (1973).
22. S. Pressel, K. S. Renzaglia, R. S. Clymo, J. G. Duckett, Hornwort stomata do not respond actively to exogenous and environmental cues. *Ann. Botany* **122**, 45–57 (2018).
23. K. S. Renzaglia, W. B. Browning, A. Merced, With over 60 independent losses, stomata are expendable in mosses. *Front Plant Sci.* **11**, 535511 (2020).
24. E. M. Ruszala *et al.*, Land plants acquired active stomatal control early in their evolutionary history. *Curr. Biol.* **21**, 1030–1035 (2011).
25. P. J. Franks, T. N. Buckley, J. C. Shope, K. A. Mott, Guard cell volume and pressure measured concurrently by confocal microscopy and the cell pressure probe. *Plant Physiol.* **125**, 1577–1584 (2001).
26. P. J. Franks, G. D. Farquhar, The mechanical diversity of stomata and its significance in gas-exchange control. *Plant Physiol.* **143**, 78–87 (2007).
27. E. A. MacRobbie, Osmotic effects on vacuolar ion release in guard cells. *Proc. Natl. Acad. Sci. U.S.A.* **103**, 1135–1140 (2006).
28. P. C. Donoghue, C. J. Harrison, J. Paps, H. Schneider, The evolutionary emergence of land plants. *Curr. Biol.* **31**, R1281–R1298 (2021).
29. B. J. Harris, C. J. Harrison, A. M. Hetherington, T. A. Williams, Phylogenomic evidence for the monophyly of bryophytes and the reductive evolution of stomata. *Curr. Biol.* **30**, 2001-2012. e2002 (2020).
30. C. Chater, J. E. Gray, D. J. Beerling, Early evolutionary acquisition of stomatal control and development gene signalling networks. *Curr. Opin. Plant Biol.* **16**, 638–646 (2013).
31. T. J. Brodribb, S. A. McAdam, Passive origins of stomatal control in vascular plants. *Science* **331**, 582–585 (2011).
32. N. Cannell *et al.*, Multiple metabolic innovations and losses are associated with major transitions in land plant evolution. *Curr. Biol.* **30**, 1783-1800. e1711 (2020).
33. C. Chater *et al.*, Regulatory mechanism controlling stomatal behavior conserved across 400 million years of land plant evolution. *Curr. Biol.* **21**, 1025–1029 (2011).
34. K. A. Shackel, E. Brinckmann, In situ measurement of epidermal cell turgor, leaf water potential, and gas exchange in Tradescantia virginiana L. *Plant Physiol.* **78**, 66–70 (1985).
35. U. Zimmermann, D. Hüsken, E.-D. Schulze, Direct turgor pressure measurements in individual leaf cells of Tradescantia virginiana. *Planta* **149**, 445–453 (1980).
36. P. M. Lintilhac, C. Wei, J. J. Tanguay, J. O. Outwater, Ball tonometry: A rapid, nondestructive method for measuring cell turgor pressure in thin-walled plant cells. *J. Plant Growth Regul.* **19**, 90–97 (2000).
37. A. J. Bidhendi, A. Geitmann, Methods to quantify primary plant cell wall mechanics. *J. Exp. Botany* **70**, 3615–3648 (2019).
38. C. Day, V. Irish, Cell ablation and the analysis of plant development. *Trends plant Sci.* **2**, 106–111 (1997).
39. S. M. Han, H. S. Baig, M. Hammarlund, Mitochondria localize to injured axons to support regeneration. *Neuron* **92**, 1308–1323 (2016).
40. P. S. Epstein, M. S. Plesset, On the stability of gas bubbles in liquid-gas solutions. *J. Chem. Phys.* **18**, 1505–1509 (1950).
41. J. Pichaco, A. Manandhar, S. A. McAdam, Mechanical advantage makes stomatal opening speed a function of evaporative demand. *Plant Physiol.* **195**, 370–377 (2024).
42. O. Heath, An experimental investigation of the mechanism of stomatal movement, with some preliminary observations upon the response of the guard cells to "shock". *New Phytol.* **37**, 385–395 (1938).
43. P. Laplace, Supplement to the tenth edition. *Méchanique céleste* **10**, 1985–1990 (1806).
44. T. Young, An essay on the cohesion of fluids. *Phil. Trans. R. Soc. Lond.* **95**, 65–87 (1805).
45. E. Steudle, J. Frensch, Water transport in plants: Role of the apoplast. *Plant soil* **187**, 67–79 (1996).
46. L. J. Voss *et al.*, Guard cells in fern stomata are connected by plasmodesmata, but control cytosolic Ca2+ levels autonomously. *New Phytol.* **219**, 206–215 (2018).
47. D. Eamus, D. T. Taylor, C. M. Macinnis-ng, S. Shanahan,L. De Silva, Comparing model predictions and experimental data for the response of stomatal conductance and guard cell turgor to manipulations of cuticular conductance, leaf-to-air vapour pressure difference and temperature: Feedback mechanisms are able to account for all observations. *Plant Cell Environ.* **31**, 269–277 (2008).
48. M. Edwards, H. Meidner, Direct measurements of turgor pressure potentials: IV. naturally occurring pressures in guard cells and their relation to solute and matric potentials in the epidermis. *J. Exp. Botany* **30**, 829–837 (1979).
49. S. A. Rensing, B. Goffinet, R. Meyberg, S.-Z. Wu, M. Bezanilla, The moss Physcomitrium (Physcomitrella) patens: A model organism for non-seed plants. *Plant Cell* **32**, 1361–1376 (2020).
50. P. Szövényi *et al.*, Establishment of Anthoceros agrestis as a model species for studying the biology of hornworts. *BMC Plant Biol.* **15**, 1–7 (2015).
51. J. Zhang *et al.*, The hornwort genome and early land plant evolution. *Nat. Plants* **6**, 107–118 (2020).
52. S. Cai *et al.*, Evolutionary conservation of ABA signaling for stomatal closure. *Plant Physiol.* **174**, 732–747 (2017).
53. W. Lauterborn, C.-D. Ohl, Cavitation bubble dynamics. *Ultrason. sonochem.* **4**, 65–75 (1997).
54. M. S. Plesset, A. Prosperetti, Bubble dynamics and cavitation. *Annu. Rev. Fluid Mech.* **9**, 145–185 (1977).
55. B.-B. Li, H.-C. Zhang, J. Lu, X.-W. Ni, Experimental investigation of the effect of ambient pressure on laser-induced bubble dynamics. *Optics Laser Technol.* **43**, 1499–1503 (2011).
56. O. Vincent, P. Marmottant, On the statics and dynamics of fully confined bubbles. *J. Fluid Mech.* **827**, 194–224 (2017).
57. M. P. Brenner, S. Hilgenfeldt, D. Lohse, Single-bubble sonoluminescence. *Rev. Modern Phys.* **74**, 425 (2002).
58. A. Edelstein, N. Amodaj, K. Hoover, R. Vale, N. Stuurman, Computer control of microscopes using μManager. *Curr. Protocols in Mol. Biol.* **92**, 14.20. 11–14.20. 17 (2010).
59. J. Schindelin *et al.*, Fiji: An open-source platform for biological-image analysis. *Nat. Methods* **9**, 676–682 (2012).
60. W. Liu *et al.*, Genome and transcriptome of Selaginella kraussiana reveal evolution of root apical meristems in vascular plants. *Curr. Biol.* **33**, 4085–4097.e4085 (2023).
61. M. C. Proctor, J. W. Bates, Chlorophyll-fluorescence measurements in bryophytes: Evidence for three main types of light-curve response. *J. Bryol.* **40**, 1–11 (2018).
62. C. R. Brodersen *et al.*, Data from "In situ cavitation bubble manometry reveals a lack of light-activated guard cell turgor modulation in bryophytes". Open Science Framework (OSF). https://osf.io/n74sk/. Deposited 24 June 2024.